



**Bidirectional cyclical flows increase energetic costs of station holding for a labriform swimming fish, *Cymatogaster aggregata***

Luongo, Sarah M.; Ruth, Andreas; Gervais, Connor R.; Korsmeyer, Keith E.; Johansen, Jacob L.; Domenici, Paolo; Steffensen, John F.

*Published in:*  
Conservation Physiology

*DOI:*  
[10.1093/conphys/coaa077](https://doi.org/10.1093/conphys/coaa077)

*Publication date:*  
2020

*Document version*  
Publisher's PDF, also known as Version of record

*Citation for published version (APA):*  
Luongo, S. M., Ruth, A., Gervais, C. R., Korsmeyer, K. E., Johansen, J. L., Domenici, P., & Steffensen, J. F. (2020). Bidirectional cyclical flows increase energetic costs of station holding for a labriform swimming fish, *Cymatogaster aggregata*. *Conservation Physiology*, 8(1), [coaa077]. <https://doi.org/10.1093/conphys/coaa077>

# Bidirectional cyclical flows increase energetic costs of station holding for a labriform swimming fish, *Cymatogaster aggregata*

Sarah M. Luongo<sup>1,\*</sup>, Andreas Ruth<sup>2</sup>, Connor R. Gervais<sup>3</sup>, Keith E. Korsmeyer<sup>4</sup>, Jacob L. Johansen<sup>5</sup>, Paolo Domenici<sup>6</sup> and John F. Steffensen<sup>2</sup>

<sup>1</sup>Department of Biological Sciences, Florida International University, 3000 N.E. 151st Street, North Miami, FL, 33181, USA

<sup>2</sup>Marine Biological Section, Department of Biology, University of Copenhagen, Strandpromenaden 5, DK-3000, Helsingør, Denmark

<sup>3</sup>Department of Biological Sciences, Macquarie University, Balaclava Rd, NSW 2109, Australia

<sup>4</sup>Department of Natural Sciences, College of Natural and Computational Sciences, Hawaii Pacific University, 1 Aloha Tower Drive, Honolulu, HI 96813, USA

<sup>5</sup>Hawaii Institute of Marine Biology, University of Hawaii at Manoa, 46-007 Lilipuna Rd, Kaneohe, HI 96744, USA

<sup>6</sup>CNR-IAS, Località Sa Mardini, 09072, Torregrande, Oristano, Italy

**\*Corresponding author:** Florida International University, Biological Sciences, 3000 N.E. 151st Street, North Miami, 33181, USA.  
Email: sarah@luongodesign.com

Wave-induced surge conditions are found in shallow marine ecosystems worldwide; yet, few studies have quantified how cyclical surges may affect free swimming animals. Here, we used a recently adapted respirometry technique to compare the energetic costs of a temperate fish species (*Cymatogaster aggregata*) swimming against a steady flow versus cyclical unidirectional and bidirectional surges in which unsteady swimming (such as accelerating, decelerating and turning) occurs. Using oxygen uptake ( $\dot{M}O_2$ ) as an estimate of energetic costs, our results reveal that fish swimming in an unsteady (i.e. cyclical) unidirectional flow showed no clear increase in costs when compared to a steady flow of the same average speed, suggesting that costs and savings from cyclical acceleration and coasting are near equal. Conversely, swimming in a bidirectional cyclical flow incurred significantly higher energetic costs relative to a steady, constant flow, likely due to the added cost of turning around to face the changing flow direction. On average, we observed a 50% increase in  $\dot{M}O_2$  of fish station holding within the bidirectional flow ( $227.8 \text{ mg O}_2 \text{ kg}^{-1} \text{ h}^{-1}$ ) compared to a steady, constant flow ( $136.1 \text{ mg O}_2 \text{ kg}^{-1} \text{ h}^{-1}$ ) of the same mean velocity. Given wave-driven surge zones are prime fish habitats in the wild, we suggest the additional costs fish incur by station holding in a bidirectional cyclical flow must be offset by favourable conditions for foraging and reproduction. With current and future increases in abiotic stressors associated with climate change, we highlight the importance of incorporating additional costs associated with swimming in cyclical water flow in the construction of energy budgets for species living in dynamic, coastal habitats.

**Key words:** Cyclical flow, oxygen uptake, respirometry, station holding, swim tunnel

**Editor:** Steven Cooke

Received 14 February 2020; Revised 12 July 2020; Editorial Decision ; Accepted 26 July 2020

**Cite as:** Luongo SM, Ruth A, Gervais CR, Korsmeyer CE, Johansen JL, Domenici P, Steffensen JF (2020) Bidirectional cyclical flows increase energetic costs of station holding for a labriform swimming fish, *Cymatogaster aggregata*. *Conserv Physiol* 00(00): coaa077; doi:10.1093/conphys/coaa077.

## Introduction

Coastal marine ecosystems typically experience dynamic, cyclical water flows (e.g. wave and tide-induced currents). Cyclical flows are beneficial for marine organisms as they transport prey and olfactory cues essential for foraging and survival and can also provide a means of passive transport for migration or dispersal (Carlson and Lauder, 2011, Fulton and Bellwood, 2005, Hart and Finelli, 1999, Webb, 1989). Individual fishes inhabiting coastal environments, however, may have to endure challenging conditions, particularly if they need to maintain position in favourable areas or avoid displacement (Carlson and Lauder, 2011, Fulton and Bellwood, 2005, Hart and Finelli, 1999, Liao, 2007). Station holding is a common behaviour seen in fishes that take advantage of specific habitats for foraging, mating and reproduction (Carlson and Lauder, 2011, Heatwole and Fulton, 2013, Webb, 1989). Species displaying station-holding behaviour often show high site fidelity above a substratum shelter and therefore must swim to accommodate daily hydrodynamic fluctuations (Carlson and Lauder, 2011, Hart and Finelli, 1999, Johansen *et al.*, 2007, Webb, 1989). Given the high number of species found in surge zones (Connell, 1978, Denny, 2006, Vijay Anand and Pillai, 2003), it has long been speculated that any excess energetic costs associated with continuous station holding must be offset by the benefits of residing in the area (Fulton and Bellwood, 2005). In addition, since swimming costs are thought to be higher in wave-swept areas (Enders *et al.*, 2003, Roche *et al.*, 2014), any adaptations to reduce elevated costs may be under strong selective pressure (Fulton *et al.*, 2013, Marcoux and Korsmeyer, 2019); furthermore, this pressure may be increasing as enhanced wind speeds, wave heights and severity of storm surge in coastal areas is expected, due to climate change (McCarthy *et al.*, 2001, Parry *et al.*, 2007, Young *et al.*, 2011). Whilst station holding can be ecologically beneficial, it also comes at a cost as resident fishes continuously have to choose between maintaining position and incurring additional energetic costs or seeking refuge from water flow (Carlson and Lauder, 2011, Johansen *et al.*, 2008, Marcoux and Korsmeyer, 2019).

Characteristics associated with dynamic flows, including changing water velocities, turbulence and oscillations in flow direction, are most pronounced in shallow, rocky reefs and shorelines (Denny, 2006, Johansen, 2014, Johansen *et al.*, 2007). In such environments, station-holding fish must continuously adjust to meet ambient surge conditions. For example, as the wave-surge increases, fish occupying the water column must accelerate and decelerate to maintain spatial position, therefore incurring an elevated demand of energy, whilst the subsequent reduction in wave-surge allows for passive coasting (Roche *et al.*, 2014). Additionally, oscillations in flow direction may require active reorientation to face the into flow (Marcoux and Korsmeyer, 2019). Conversely, demersal species (i.e. species associated with the seafloor) may exhibit morphological and behavioural traits

allowing them to reduce exposure to ambient hydrodynamics, by refuging and residing near the substrate (Johansen *et al.*, 2008, Johansen *et al.*, 2007, Webb, 1989).

Energetic costs of swimming have been determined by measuring oxygen uptake rates (Nelson, 2016, Roche *et al.*, 2014, Svendsen *et al.*, 2016); however, standard swimming performance experiments are predominantly examined using stepwise changes in velocity with constant flows (Beamish, 1964, Brett, 1964, Brett, 1972, Brett, 1971, Kramer and McLaughlin, 2001, Liao, 2007, Marras *et al.*, 2015, Steffensen *et al.*, 1984), which does not account for additional energetic costs associated with swimming in flow regimes with varying velocities (Enders *et al.*, 2003, Liao, 2007, Marcoux and Korsmeyer, 2019, Roche *et al.*, 2014). More recently, studies have included metabolic estimates of fish swimming in turbulent or cyclic flows. For example, Enders *et al.* (2003) determined that forced swimming models underestimate the true costs of swimming in turbulent flow by two to 4-fold for juvenile Atlantic salmon (*Salmo salar*). A study by van der Hoop *et al.* (2018) found a reduction in oxygen uptake by a temperate labriform swimmer, the shiner perch (*Cymatogaster aggregata*), when it experienced highly turbulent flow suggesting that fish may also be able to take advantage of the physical properties of uneven flow regimes to decrease energetic costs if refuge is not available. In addition, Roche *et al.* (2014) found that when *C. aggregata* was exposed to a cyclical flow treatment (consisting of a repeatable, unidirectional surge), they incurred an increase in energetic costs by 25.3% when compared to constant flow treatments at the same mean speed (Roche *et al.*, 2014). However, many natural surge habitats are exposed to bidirectional flows in which the flow periodically reverts its direction. In such types of flow, fish must make a whole-body rotation whilst maintaining position to continuously face the direction of the flow (Blake and Chan, 2010, Hamner *et al.*, 1988, Heatwole and Fulton, 2013). Fulton and Bellwood (2005) showed that median-paired fin (MPF *sensu* Webb 1984) swimming fishes (i.e. those swimming predominantly with the dorsal, anal or pectoral fins) were most abundant in tropical coral reef environments with high, wave-induced water velocities, suggesting that these fish are better suited to manoeuvre and withstand dynamic conditions. Indeed, Marcoux and Korsmeyer (2019) recently measured how energetic costs differ amongst four types of swimming modes for tropical coral reef fishes station holding in bidirectional, oscillatory flow conditions. The costs of swimming in the median-paired fin swimmers (*Sufflamen bursa* and *Ctenochaetus strigosus*) were less affected by increases in the frequency of bidirectional flow than that of axial swimmers (*Kuhlia xenura* and *Kuhlia sandvicensis*) using undulations of the body and caudal fin, confirming that non-body locomotion (i.e. MPF swimming) may be more favourable in reef habitats or areas with high amounts of wave-surge (Marcoux and Korsmeyer, 2019). Accordingly, Schakmann *et al.* (2020) recently compared the net costs of swimming of a tropical, coral reef fish *C. strigosus*, in a steady, unidirectional and bidirectional flow regimes

of varying frequencies and amplitudes, concluding that the costs of station holding in a bidirectional flow increase 2-fold compared to steady flow, potentially driven by the physical act of turning. Whilst this study was a major advance in current knowledge about energetic costs of swimming in wave-driven, cyclical flow environments, this is a virtually unexplored topic of research across species, ecosystems and latitudes, and its impact on animal energy budgets and species distributions remains uncertain.

In the present study, we measured swimming costs of a temperate species in simulated wave-driven water movements, similar to the surge regime experienced by coastal fishes, and compared how these costs differed from costs incurred in a steady, constant flow. We used *C. aggregata* as a model species due to its natural occurrence in coastal surge areas (Roche *et al.*, 2014, Shaw and Allen, 1977). Water flows were generated from standardized, repeatable, sinusoidal wave functions, one with periodic reversals in flow (bidirectional cyclical flow), and a similar velocity function with flows in only one direction (i.e. unidirectional cyclical flow). Additionally, we calculated two predicted values for both cyclical flows, which were used to isolate the energetic costs of certain behaviours (i.e. accelerating, decelerating and turning) associated with swimming in cyclical flow regimes.

This study tested the following main hypotheses in terms of the energetic cost of swimming in the three treatments (steady, unidirectional and bidirectional flow): (i) fish swimming in a uni- or bidirectional cyclical flow have a predicted  $\dot{M}O_2$  ( $\dot{M}O_{2,P1}$ ) that corresponds to that calculated based on swimming at a constant speed (i.e. at the absolute mean flow velocity of the uni- and bidirectional cyclical treatments), implying no additional costs of accelerating, decelerating and turning; (ii) fish swimming in a uni- or bidirectional cyclical flow have a predicted  $\dot{M}O_2$  ( $\dot{M}O_{2,P2}$ ) that corresponds to the  $\dot{M}O_2$  of fish in the steady, constant flow treatment integrated over the entire velocity cycle, implying that accelerating, decelerating and turning cause additional energetic costs; (iii) fish swimming in a bidirectional flow incur additional aerobic energetic costs compared to swimming in a unidirectional flow, caused by turning to maintain position and direction against the flow.

## Methods

### Experimental animals and husbandry

*Cymatogaster aggregata* ( $n = 7$ , steady speed treatment;  $n = 11$  repeated measures for uni- and bidirectional treatments; total length =  $11.72 \pm 0.36$  cm; mass =  $21.37 \pm 1.75$  g; mean  $\pm$  s.d.) were caught using a beach seine on San Juan Island, Washington, USA ( $48^\circ 32'N$   $123^\circ 05'W$ ) during August 2017. Fish were held at the Friday Harbor Laboratories of the University of Washington in flow-through tanks, supplied by natural seawater (mean  $\pm$  s.d., temperature,  $12.8 \pm 1.2^\circ C$ ; salinity, 34 ppt) and held under a natural light regime (16:8 h). No additional food was provided during husbandry—however,

fish fed freely on plankton in the water. Fish habituated in husbandry tanks for at least 24 h prior experimental trials. All methods were approved by the Institutional Animal Care and Use Committee at the University of Washington (IACUC protocol number 4238-03).

### Experimental setup

Swimming performance and oxygen uptake rates were measured by intermittent flow-respirometry in a 8.45 L of clear acrylic, Steffensen-type swimming respirometer (Methling *et al.*, 2011, Steffensen *et al.*, 1984), with a working section of  $9.0 \times 26.0 \times 10.0$  cm (width  $\times$  length  $\times$  depth), and a flow straightener added to the downstream end of the working section. The respirometer was immersed in a 35.8 L of experimental tank connected to an aerated 81 L of water sump, and water was circulated through a UV filter (TetraPond 19 520, 120 V, 60 Hz; 9.8 W) to minimize microbial respiration and reduce background oxygen uptake. Additionally, the chamber was cleaned with a bleach solution every 2 days to remove microbial growth.

Water oxygen tension was measured with a fibre optic oxygen sensor (Fibox 3, Precision Sensing GmbH, Regensburg, Germany). The zero calibration was done in a mixture of sodium thiosulfate and a pinch of Borax (sodium borate). All oxygen tension measurements were monitored and logged with AutoResp V1 (Loligo Systems, Copenhagen, Denmark). Temperature was maintained at  $13.0 \pm 0.1^\circ C$  (mean  $\pm$  s.d.) and regulated by a programmable relay (PR-5714D, PR Electronics, Denmark), which controlled a submersible Eheim pump in connection with a cooling unit (Lauda Brinkmann, RM20 refrigerating circulating bath).

Water velocity and direction (unidirectional and bidirectional) were continuously controlled by Labtech Notebook (<https://www.omega.com/>), via an analogue output to a motor-unit (Movitrac AC VFD, SEW EURODRIVE, Lyman, SC, USA) via an ADDA converter (Measurement Computing). Solid blocking effects of the trial fish in the swimming respirometer were corrected according to Bell and Terhune (1970).

### Water velocity calibration

Water velocity (cm/s) in a constant, microturbulent flow was calibrated using a digital flow meter (TAD W30, Höntzsch, Waiblingen, Germany). The digital flow meter was inserted in the working section of the swim tunnel at three different levels (bottom, middle and top) to ensure homogenous water velocity throughout the working area. Starting from a static system, the motor voltage (V) was increased, and the corresponding flow was recorded every 0.5 V.

The water velocity throughout the unidirectional and bidirectional wave cycles was analyzed and calibrated using digital particle image velocimetry (DPIV) to generate a velocity curve over an entire flow period. A 532-nm, 50-mW laser

**Table 1:** Water flow characteristics of the unidirectional and bidirectional flow regimes; the period for both flow regimes was 5 s (frequency = 0.2 Hz)

Water flow regime	Minimum speed (BL s <sup>-1</sup> )	Mean speed (BL s <sup>-1</sup> )	Maximum speed (BL s <sup>-1</sup> )	Amplitude (BL s <sup>-1</sup> )
Unidirectional	1.41	1.87	2.14	0.73
Bidirectional	0.00	1.39	2.18	2.18

line module locator (Laserland, Besram Technologies) was mounted above the swim flume and illuminated a thin sheet along the working area. Video was captured at 120 frames per second (FPS) at 640 × 480 pixels with an Olympus TG-4 (Olympus Australia Pty Ltd, Macquarie Park, NSW).

*Artemia* cysts (Sander's Premium Great Salt Lake *Artemia* Cysts) were used as neutrally buoyant tracer particles for the DPIV measurements. The cysts were prepared by soaking for 40 min (Lauder and Clark, 1984), after which cysts at the surface were removed and the solution of neutrally buoyant cysts were added to the swim tunnel. Images for DPIV were analyzed using Logger Pro (Vernier, Beaverton, OR). Three particles per frame were tracked over three continuous frames (three frames, 0.025 s) over three entire flow period (5 s; 600 frames) for each dynamic flow (uni- and bidirectional). Velocity was calculated by averaging the distance the particle travelled over each measurement period across the top, middle and bottom of the swim tunnel. A description of each flow regime is described in Equations (3) to (4) below (Table 1, Fig. 1 and Supplementary Figure 1).

## Oxygen uptake

Oxygen uptake rates ( $\dot{M}O_2$ : mg O<sub>2</sub> kg<sup>-1</sup> h<sup>-1</sup>) were used as a proxy for oxidative metabolism at various swimming speed regimes (Beamish, 1964, Chabot *et al.*, 2016, Nelson, 2016). The  $\dot{M}O_2$  was calculated from the linear regression of the decline in oxygen tension as function of time (Steffensen *et al.*, 1984, Svendsen *et al.*, 2016):

$$\dot{M}O_2 = \alpha \Delta O_2 V_{\text{resp}} M_{\text{fish}}^{-1} \quad \text{Equation (1)}$$

where  $\Delta O_2$  is the slope of the decline in oxygen partial pressure as function of time,  $\alpha$  is the oxygen solubility of the water,  $V_{\text{resp}}$  is the volume of the respirometer minus the volume of the fish (L) assuming the density of the water equals the density of the fish (Green and Carritt, 1967) and  $M_{\text{fish}}$  is the mass of the fish. Microbial (i.e. background) respiration was determined prior and after each measurement trial with an extended measurement phase of 30 min and the average subtracted from  $\dot{M}O_2$  measurements of the corresponding fish.

## Experimental protocol

To ensure enough space for the fish to turn within the working chamber of the respirometer in the bidirectional flow treatment, the dimensions of the respirometer were at

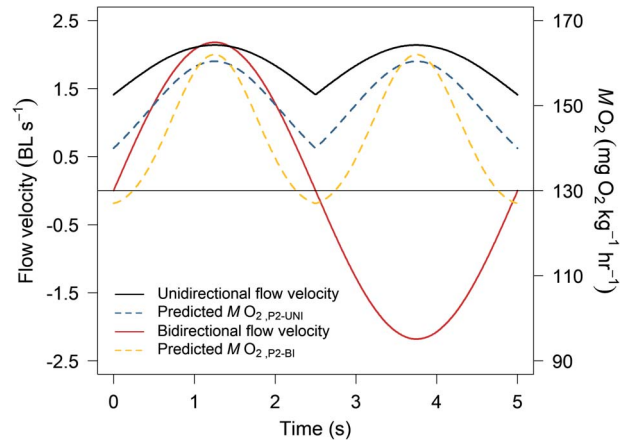


**Figure 1:** Unidirectional (solid black line) and bidirectional (solid red line) flow and predicted oxygen uptake rates ( $\dot{M}O_{2,P2}$ ) (wave period = 5 s). The unidirectional flow is described as  $y = |0.73\sin(2\pi 0.2 t)| + 1.41$  and the bidirectional flow is described as  $y = 2.18\sin(2\pi 0.2 t)$ . Predicted oxygen uptake rates are presented over the cyclical changes in velocity for both uni- ( $\dot{M}O_{2,P2-UNI}$ ; dashed blue line) and bidirectional ( $\dot{M}O_{2,P2-BI}$ ; dashed gold line) flows. Predicted values were calculated by integrating the sinusoidal equation [Equation (3)] and the modified sinusoidal equation [Equation (4)] into the power function for  $\dot{M}O_2$  and constant swimming speed [ $U$ ; Equation (2)], thus producing Equations (7) and (8), respectively. Mean  $\dot{M}O_{2,P2-UNI}$  and mean  $\dot{M}O_{2,P2-BI}$  were used for comparison to the uni- and bidirectional  $\dot{M}O_2$  measurements (Table 2)

least 14 cm longer than the average fish in the chamber, and the length of the fish was no more than 23% longer than the width of the flume. Given that the fish bends to turn, this ensured sufficient space and preliminary observations of fish in the bidirectional flow confirmed this; however, the mean respirometer:organism volume-ratio was, on average, 398:1, thereby exceeding the recommendations (<150:1) for swimming respirometers according to Svendsen *et al.* (2016). Therefore, to ensure linear decline (with an  $r^2 \geq 0.86$ ) of oxygen as a function of time, oxygen uptake rates were determined from a series of continuously, intermittent measurement cycles, consisting of a 900-s measurement phase, followed by a 240-s flush and 60-s mixing phase.

## Unidirectional swimming at steady velocities

$\dot{M}O_2$  [Equation (2)] at steady, unidirectional water flow velocities was established following a modified standard critical swimming speed protocol ( $U_{\text{crit}}$ ; Table 2 and Fig. 2)



**Table 2:** Individual results of the three-parameter hydrodynamic power function [Equation (2);  $\dot{M}O_2 = a + b \cdot U^c$ ] for each of the seven fish that underwent the modified  $U_{crit}$  protocol ( $\pm$  s.e.).  $\dot{M}O_{2,P1}$  values for uni- and bidirectional flow were calculated from Equations (5) to (6), respectively (mean  $\pm$  s.d.).  $\dot{M}O_{2,P2}$  values for uni- and bidirectional flow were calculated from Equations (7) to (8), respectively (mean  $\pm$  s.d.)

Fish	TL (cm)	Power function parameters			Unidirectional		Bidirectional	
		a	b	c	$\dot{M}O_{2,P1}$	$\dot{M}O_{2,P2}$	$\dot{M}O_{2,P1}$	$\dot{M}O_{2,P2}$
1	12.5	144.8 $\pm$ 7.5	0.1 $\pm$ 0.4	5.9 $\pm$ 3.4	148.7	149.6 $\pm$ 2.7	145.5	147.8 $\pm$ 3.5
2	12.0	82.8 $\pm$ 8.2	19.6 $\pm$ 8.2	1.2 $\pm$ 0.3	125.3	125.5 $\pm$ 6.3	112.2	113.3 $\pm$ 16.8
3	11.0	124.3 $\pm$ 4.5	2.7 $\pm$ 2.0	3.0 $\pm$ 0.7	142.4	143.3 $\pm$ 6.3	131.7	136.4 $\pm$ 10.5
4	11.7	119.7 $\pm$ 15.5	10.5 $\pm$ 12.1	2.0 $\pm$ 1.0	156.5	171.1 $\pm$ 9.5	140.0	157.4 $\pm$ 19.4
5	11.8	120.6 $\pm$ 9.5	8.3 $\pm$ 6.2	2.4 $\pm$ 0.7	156.5	157.5 $\pm$ 9.9	138.5	144.7 $\pm$ 18.6
6	11.5	149.2 $\pm$ 2.4	2.2 $\pm$ 0.7	3.3 $\pm$ 0.3	166.5	172.4 $\pm$ 2.9	155.7	170.5 $\pm$ 3.8
7	11.7	119.5 $\pm$ 7.1	3.5 $\pm$ 3.1	3.1 $\pm$ 0.8	143.3	144.6 $\pm$ 8.4	129.1	135.5 $\pm$ 13.9
Mean	11.7 $\pm$ 0.5	123.0 $\pm$ 21.6	6.7 $\pm$ 6.7	3.0 $\pm$ 1.5	148.4 $\pm$ 13.2	152.0 $\pm$ 16.6	136.1 $\pm$ 13.7	143.7 $\pm$ 18.1

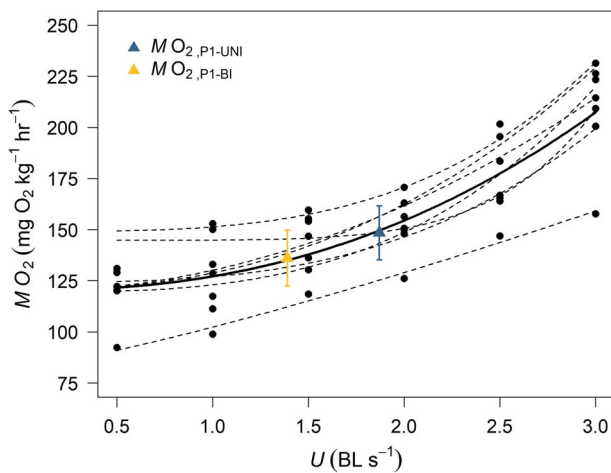


**Figure 2:** Oxygen uptake rate ( $\dot{M}O_2$ ;  $\text{mg O}_2 \text{ kg}^{-1} \text{ h}^{-1}$ ) in relation to swimming speed for *Cymatogaster aggregata* ( $n = 7$ ) in constant flow (mean  $\pm$  s.d.), fit to a power function:  $\dot{M}O_2 = 120.27 \pm 7.12 + 6.92 \pm 4.70 U^{2.31 \pm 0.59}$ ,  $r^2 = 0.75$ . Black dashed lines represent individual power functions for each of the seven fish (Table 2) and black circles represent the mean  $\dot{M}O_2$  of each fish at the corresponding speed.  $\dot{M}O_{2,P1-UNI}$  (blue triangle; mean  $\pm$  s.d.,  $148.4 \pm 13.2 \text{ mg O}_2 \text{ kg}^{-1} \text{ h}^{-1}$ ), and  $\dot{M}O_{2,P1-BI}$  (gold triangle; mean  $\pm$  s.d.,  $136.1 \pm 13.7 \text{ mg O}_2 \text{ kg}^{-1} \text{ h}^{-1}$ ) are the mean  $\dot{M}O_2$  values at the same absolute mean swimming speed for uni- and bidirectional cyclical flow treatments, 1.87 and 1.39  $\text{BL s}^{-1}$ , respectively. The  $r$ -squared value for the power function was calculated by subtracting the sum of squares of the data from the sum of squares of the residuals and subtracting it from one

(Brett, 1964). Prior to each swimming trial, individual fish were introduced to the respirometer and allowed to habituate at a steady flow velocity of 0.5  $\text{BL s}^{-1}$ , until  $\dot{M}O_2$  stabilized, typically between 3 and 4 h (Chabot *et al.*, 2016, Roche *et al.*, 2014). Water flow velocity ( $U$ ) was incrementally increased by 0.5  $\text{BL s}^{-1}$  following every third measurement cycle. Swimming speeds were selected below gait-transitioning

( $U_{p-c}$ ) to ensure fish were demonstrating aerobic swimming (Roche *et al.*, 2014). Measurements were stopped after three measurements at  $U = 3.0 \text{ BL s}^{-1}$ , and all individuals were transferred to their holding tanks. No fish were observed to fatigue at any of the flow velocities examined. To avoid overuse of the fish, the seven fish that underwent the modified  $U_{crit}$  protocol were not used in the cyclical flow treatments.

A three-parameter, hydrodynamic-based power function was fit to  $\dot{M}O_2$  as a function of swimming speed ( $U$ ) (Korsmeyer *et al.*, 2002) for the constant flow swimming protocol. The relationship is described by the following Equation (2):

$$\dot{M}O_2 = a + b \cdot U^c \quad \text{Equation (2)}$$

where  $a$  is equal to the theoretical oxygen uptake at standard metabolic rate (SMR) at zero speed ( $\dot{M}O_{2,SMR}$ ),  $b$  is the linear coefficient and  $c$  is the power to which water flow velocity,  $U$ , is raised.

### Uni- and bidirectional swimming treatments at varying velocities

A computer-generated sine-wave function [Equation (3)] simulated moderate wave periods (5 s) representative of those found in the San Juan Islands, Washington, inshore coasts (Finlayson, 2006, Roche *et al.*, 2014) (Fig. 1). The sinusoidal oscillation in velocity over time is described by the following Equation (3):

$$U(t) = \alpha \cdot \sin(2\pi ft) \quad \text{Equation (3)}$$

where  $U$  is the water velocity as function of time  $t$  (s),  $f$  is the frequency (0.2 Hz) and  $\alpha$  equals the velocity amplitude ( $\text{BL s}^{-1}$ ) during the sinusoidal wave. Using this equation, we attempted to create two different cyclic flow regimes:

(i) applying the sinusoidal wave function properties to the flow regime, the velocity follows a sine wave with half the period in one direction (positive) and the other half in the opposite direction (negative) with the velocity crossing zero every 2.5 s (Finlayson, 2006) (hereafter referred to as bidirectional cyclical flow; Fig. 1, red line); and (ii) taking the absolute value of the sinusoidal wave function [Equation (3)] thereby generating all velocities in the same direction with the velocity approaching zero every 2.5 s (hereafter referred to as unidirectional cyclical flow; Fig. 1, black line). Both the uni- and bidirectional flow regimes were programmed to have an amplitude corresponding to  $\sim 70\%$  of  $U_{crit}$  for *C. aggregata* ( $\sim 3.0 \text{ BL s}^{-1}$ ) therefore ensuring that maximum speeds did not cause anaerobically driven gait transitioning in this species (Roche *et al.*, 2014). Flow calibration confirmed that the unidirectional flow obtained a mean amplitude of  $0.73 \pm 0.05 \text{ BL s}^{-1}$  ( $\pm \text{ s.e.}$ ) and a maximum speed of  $2.14 \text{ BL s}^{-1}$  whilst the bidirectional flow obtained an amplitude and maximum speed of  $2.18 \pm 0.03 \text{ BL s}^{-1}$  ( $\pm \text{ s.e.}$ , Table 1). Lastly, the combined effects of inertial forces and the duration of the wave period did not allow the unidirectional flow to completely stop at zero, as described by Equation (4) (Schakmann *et al.*, 2020):

$$U(t) = |\alpha \cdot \sin(2\pi ft)| + e \quad \text{Equation (4)}$$

where  $U$  is the water velocity as function of time  $t$  (s),  $f$  is the frequency (0.2 Hz) and  $\alpha$  equals the amplitude ( $\text{BL s}^{-1}$ ) above the elevation ( $e$ ) and  $e$  is the elevation of the waveform above zero, corresponding to the minimum speed ( $\text{BL s}^{-1}$ ) (Schakmann *et al.*, 2020). Characteristics of the uni- and bidirectional flow regimes are described in Table 1.

To ensure there was no confounding effect of treatment order, each individual experienced both the unidirectional and bidirectional treatments and were randomly assigned that treatment they would experience first. Oxygen uptake rates were measured through three measurement cycles for one treatment (for a total of 1 h), before returning to the initial constant flow ( $0.5 \text{ BL s}^{-1}$ ). The fish was then allowed to settle down for 1 h and restore their baseline  $\dot{M}\text{O}_2$  (steady state), before being exposed to the other cyclical flow treatment for an additional three measurement cycles. Finally, to ensure our results were not driven by a learning behaviour of the fish (i.e. improving in performance over time) for three individual fish that ended on the bidirectional measurement, we conducted extended measurements of oxygen consumption in a subset of individuals (see Supplementary Figure 2).

### Predicted oxygen uptake rates

Measured rates of oxygen uptake during the cyclical flow treatments were each compared with the two predicted values:

(1) The first predicted value ( $\dot{M}\text{O}_{2,P1}$ ) was based on the assumption that, if there are no additional costs associated

with the varying speeds and flow directions of the uni- or bidirectional flow cycles, then a fish in either treatment would exhibit the same  $\dot{M}\text{O}_2$  as that measured at the same absolute mean velocity of the steady, constant flow, from the modified  $U_{crit}$  protocol. To calculate this value for each cyclical flow, we first generated a three-parameter hydrodynamic power function [Equation (2)] for each of the seven fish that experienced the modified  $U_{crit}$  protocol (Fig. 2, black dashed lines). The average absolute water velocity for the unidirectional flow and bidirectional flow were calculated using the equations,  $\alpha \cdot 2/\pi + e$  and  $\alpha \cdot 2/\pi$ , respectively (Table 1). As a result,  $\dot{M}\text{O}_{2,P1}$  was calculated for both the uni- and bidirectional flow characteristics:

$$\dot{M}\text{O}_{2,P1-UNI} = a + b \cdot (\alpha \cdot 2/\pi + e)^c \quad \text{Equation (5)}$$

$$\dot{M}\text{O}_{2,P1-BI} = a + b \cdot (\alpha \cdot 2/\pi)^c \quad \text{Equation (6)}$$

The first predicted value for each flow,  $\dot{M}\text{O}_{2,P1-UNI}$  and  $\dot{M}\text{O}_{2,P1-BI}$  was derived from the mean  $\dot{M}\text{O}_2$  of the seven fish at the mean swimming speed of the uni- and bidirectional flows, respectively. The first set of predicted values tested the hypothesis that there are no additional costs of swimming in cyclical flows compared with steady swimming at the same average speed.

(2) The second predicted value ( $\dot{M}\text{O}_{2,P2}$ ) was based on the mean  $\dot{M}\text{O}_2$  of a fish that corresponds to the all the speeds encountered during the uni- and bidirectional flow cycle as determined in the stepwise, constant speed ( $U_{crit}$ ) modified protocol [Fig. 1, dashed blue (unidirectional) and gold (bidirectional) lines]. This was achieved by integrating the area under the curve of the hydrodynamic power function [Equation (2)], generated from the relationship between  $U$  and  $\dot{M}\text{O}_2$  (Fig. 2), over the sinusoidal changes in velocity of the uni- and bidirectional flows [Equations (3) to (4), respectively] for each of the seven fish. The  $\dot{M}\text{O}_2$  at a given time during the cycle was calculated as follows:

$$\dot{M}\text{O}_{2,P2-UNI}(t) = a + b \cdot (|\alpha \cdot \sin(2\pi ft)| + e)^c \quad \text{Equation (7)}$$

$$\dot{M}\text{O}_{2,P2-BI}(t) = a + b \cdot (\alpha \cdot \sin(2\pi ft))^c \quad \text{Equation (8)}$$

The resulting  $\dot{M}\text{O}_2$  values for each flow [Fig. 1, dashed blue (unidirectional) and gold (bidirectional) lines] were averaged over a complete cycle for each fish, and a mean was calculated for each flow, providing us with the second predicted  $\dot{M}\text{O}_{2,P2}$  of fish in the cyclic flow treatments,  $\dot{M}\text{O}_{2,P2-UNI}$  and  $\dot{M}\text{O}_{2,P2-BI}$ . Therefore, these theoretical values were used to test the hypothesis that fish in the uni- and bidirectional flow treatments have costs equivalent to swimming at steady speeds over the range of cyclic velocities experienced, accounting for the non-linear relationship between  $\dot{M}\text{O}_2$  and speed,

but incur no additional costs of accelerating, breaking and, in the bidirectional flow, turning.

## Data analysis

A two-sample *t*-test was used to compare  $\dot{M}O_2$  of the uni- and bidirectional cyclical flow treatments to each of their respective predicted values ( $\dot{M}O_{2,P1-UNI}$ ,  $\dot{M}O_{2,P2-UNI}$ ,  $\dot{M}O_{2,P1-BI}$  and  $\dot{M}O_{2,P2-BI}$ ).  $\dot{M}O_{2,P1}$  and  $\dot{M}O_{2,P2}$  values for each fish and each cyclical flow regime were generated from the individual power functions of the fish that underwent a modified  $U_{crit}$  protocol (Table 2). All statistical analyses were completed using R (version 3.2.2) (R Core Team, 2016).

## Results

### Steady velocity swimming and predicted oxygen uptake rates

The three-parameter hydrodynamic-based power function describing the relationship between oxygen uptakes ( $\dot{M}O_2$ ) as a function of swimming speed ( $U$ ) in the modified  $U_{crit}$  protocol ( $0.5\text{--}3\text{ BL s}^{-1}$ ; Fig. 2, solid black line;  $R^2 = 0.75$ ) for all fish ( $n = 7$ ) was:

$$\dot{M}O_2 = 120.27 \pm 7.12 + 6.92 \pm 4.70 U^{2.31 \pm 0.59} \quad \text{Equation (9)}$$

The mean  $\dot{M}O_{2,P1}$  at the average absolute swimming velocity for the unidirectional and bidirectional flow was  $148.4 \pm 13.2$  and  $136.1 \pm 13.7\text{ mg O}_2\text{ kg}^{-1}\text{ h}^{-1}$ , respectively (mean  $\pm$  s.d.; Table 2, Figs 2 and 3). The predicted mean  $\dot{M}O_{2,P2}$  for the unidirectional and bidirectional flow was  $151.1 \pm 16.6$  and  $143.7 \pm 18.1\text{ mg O}_2\text{ kg}^{-1}\text{ h}^{-1}$ , respectively (mean  $\pm$  s.d.; Table 2, Fig. 3).

### Uni- and bidirectional swimming treatments at varying velocities

There were no significant differences between  $\dot{M}O_2$  in the unidirectional flow ( $154.7 \pm 19.5\text{ mg O}_2\text{ kg}^{-1}\text{ h}^{-1}$ , mean  $\pm$  s.d.) compared to both  $\dot{M}O_{2,P1-UNI}$  (two sample *t*-test;  $t = 0.816$ ,  $df = 15.86$ ,  $P = 0.42$ ) and  $\dot{M}O_{2,P2-UNI}$  (two sample *t*-test;  $t = 0.321$ ,  $df = 14.473$ ,  $P = 0.75$ ) (Fig. 3). However, there were significant differences between the  $\dot{M}O_2$  in the bidirectional flow ( $227.8 \pm 29.1\text{ mg O}_2\text{ kg}^{-1}\text{ h}^{-1}$ , mean  $\pm$  s.d.) compared to both  $\dot{M}O_{2,P1-BI}$  (two sample *t*-test;  $t = 9.005$ ,  $df = 15.134$ ,  $P < 0.001$ ) and  $\dot{M}O_{2,P2-BI}$  (two sample *t*-test;  $t = 7.564$ ,  $df = 15.999$ ,  $P < 0.001$ ), with an increase of 50 and 45%, respectively (Fig. 3).

## Discussion

Through the use of a recently adapted respirometry technique, we demonstrate the importance of incorporating dynamic, cyclical flow regimes when estimating energetic costs of

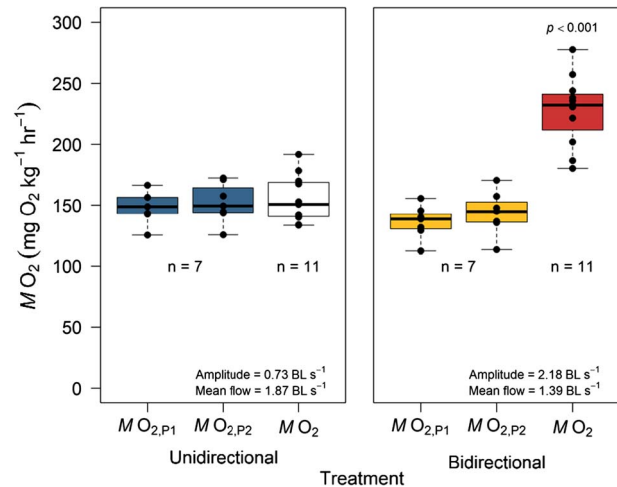


**Figure 3:** Oxygen uptake rate ( $\dot{M}O_2$ ;  $\text{mg O}_2\text{ kg}^{-1}\text{ h}^{-1}$ ) for unidirectional and bidirectional cyclic flow treatments ( $n = 11$ ) compared to the two predicted values for each treatment ( $n = 7$ ). Boxes represent the first- and third quartiles; bold lines indicate median values. Whiskers denote variability outside of the quartiles and open circles represent outliers. Black circles represent individual values for each fish.  $\dot{M}O_{2,P1}$  values for each flow regime are generated from the assumption that fish in a cyclical flow would have the same  $\dot{M}O_2$  at the same absolute mean swimming speed as in a stepwise constant flow [Equations (5) to (6), respectively]. Mean  $\dot{M}O_{2,P2}$  values for each flow regime are derived from integrating the modified sinusoidal wave function in the hydrodynamic power function for  $\dot{M}O_2$  [Equation (7) to (8), respectively]. There was no significant difference between  $\dot{M}O_2$  of the unidirectional flow compared to either predicted value; however, there was a significant difference between  $\dot{M}O_2$  of the bidirectional flow compared to both predicted values ( $P < 0.001$ ).

species living in coastal environments (Liao, 2007, Marcoux and Korsmeyer, 2019, Schakmann *et al.*, 2020, Webb, 1984). Most open shorelines rarely experience prolonged periods of still water or constant flows as wind-driven oscillatory waves, varying in frequency and amplitude, are ubiquitous to coastal environments (Fulton and Bellwood, 2005, Fulton *et al.*, 2013, Marcoux and Korsmeyer, 2019, Schakmann *et al.*, 2020). Assuming that fishes living in coastal, intertidal environments only swim at steady speeds is therefore likely to misrepresent the true costs of swimming (Roche *et al.*, 2014, Webb, 1989). Here, we found *C. aggregata* may incur a 50% ( $91.7\text{ mg O}_2\text{ kg}^{-1}\text{ h}^{-1}$ ) increase in oxygen uptake for station holding in a bidirectional cyclical flow compared to swimming in a steady flow with the same mean velocity ( $\dot{M}O_{2,P1-BI}$ ). Fish in the unidirectional flow, which had to constantly accelerate and decelerate to overcome inertia, without changing their orientation, did not have significantly increased costs compared to steady swimming at the same mean velocity ( $\dot{M}O_{2,P1-UNI}$ ,  $<5\%$ ) or accounting for the range of velocities ( $\dot{M}O_{2,P2-UNI}$ ,  $<2\%$ ). Therefore, we can assume that costs associated with accelerating are either negligible or the savings associated with coasting/decelerating offset the cost of acceleration. Based on this result, the excess energetic



costs of swimming in a bidirectional cyclical flow are likely predominantly driven by the cost of turning as the fish is continuously required to physically turn around and reorient itself as water direction changes (Schakmann *et al.*, 2020).

It is difficult to quantify the costs associated with constant swimming and manoeuvring of wild fish displaying a station-holding behaviour in hydrodynamic environments (Carlson and Lauder, 2011, Hart and Finelli, 1999, Johansen *et al.*, 2007, Webb, 1989); however, continuous acceleration and deceleration associated with swimming in a cyclical wave surge is believed to be more energetically costly than maintaining a constant swimming speed (Heatwole and Fulton, 2013, Marcoux and Korsmeyer, 2019, Roche *et al.*, 2014). Surprisingly, our results revealed this not to be true, supporting the findings from Schakmann *et al.* (2020), which did not find a significant increase in the net costs of swimming for *C. strigosus* in a unidirectional, cyclical flow. One possible explanation for this could be because fish in the unidirectional cyclical flow may exert additional energy to accelerate with increasing flow velocity but then conserve energy whilst decelerating as the flow decreases, therefore allowing these two parts of the wave cycle to energetically offset one another (Marcoux and Korsmeyer, 2019, Schakmann *et al.*, 2020). Furthermore, Roche *et al.* (2014) concluded *C. aggregata* would decrease the number of fin beats during the deceleration phase therefore transitioning into a gliding behaviour and conserving energy. By comparing our unidirectional measurement to that predicted from steady swimming costs over the cycle ( $\dot{M}O_{2,P2-UNI}$ ), we were able to determine that the costs of continuously accelerating and breaking to overcome inertia were not significantly different from the costs to overcome drag at the velocities experienced during the wave cycle. Our findings are in contradiction to Roche *et al.* (2014) who found a 14.2% increase between predicted  $\dot{M}O_2$  representative of the non-linear relationship between oxygen uptake and swimming speed (equivalent to our  $\dot{M}O_{2,P2-UNI}$ ) and their unidirectional cyclical flow at high amplitude ( $1.0 \text{ BLs}^{-1}$ ), indicating an added cost of the acceleration and deceleration. One possible explanation for the differences between our findings and those of Roche *et al.* (2014) could be the fish in our study were smaller, being on average 24% shorter (TL) and weighing 74% less, and therefore experiencing less drag due to their smaller surface area. Our study required relatively small fish that were able to turn around in the chamber for the bidirectional cyclical flow treatment without interacting with the surrounding sides of the respirometer. This may have aided in energy conservation as fish in our study had a slightly larger working area (i.e. an extra  $\sim 0.5$  body lengths) with which they could decelerate whilst the larger fish used by Roche *et al.* (2014) may also have used more energy (i.e. higher  $\dot{M}O_2$ ) because of their higher inertia and need for active deceleration/breaking to maintain station holding with a smaller swimming section of the respirometer.

Although the comparison between  $\dot{M}O_2$  of fish in the unidirectional flow and the bidirectional flow needs to be

done with caution, due to the differences in flow characteristics (Table 1), a few distinctions are worth discussing. The unidirectional flow had a higher mean swimming speed than the bidirectional flow; yet, the  $\dot{M}O_2$  of swimming in the bidirectional flow was 47% greater. Therefore, our estimates of costs associated with turning are likely to be conservative. Additionally, whilst this study measured  $\dot{M}O_2$  at a single frequency and amplitude (Table 1), our results are supported by a previous study on a tropical reef fish using additional frequencies and amplitudes (Schakmann *et al.*, 2020). Specifically, Schakmann *et al.* (2020) also found costs associated with accelerating and decelerating to be negligible relative to the costs of turning  $180^\circ$  whilst station holding in bidirectional, cyclical flows.

Species that are morphologically or behaviourally adapted for minimizing costs in complex and dynamic water flows are expected to be most prevalent in coastal and coral reef-type ecosystems (Fulton *et al.*, 2013, Marcoux and Korsmeyer, 2019). *Cymatogaster aggregata* are pectoral fin, or labriform, swimmers (Roche *et al.*, 2014), and therefore based on findings from Marcoux and Korsmeyer (2019) are less sensitive to increases in wave frequency or direction changes in wave-surge habitats compared with fishes using swimming modes involving body and caudal fin undulations (Blake, 2004, Fulton, 2007, Marcoux and Korsmeyer, 2019, Webb, 1994). This conclusion is consistent with previous studies that have found fishes with the pectoral fin swimming mode to be predominate in coral reef ecosystems exposed to high wave action (Fulton and Bellwood, 2005, Fulton *et al.*, 2013). For species in coastal habitats that experience dynamic water flow, increased fitness may be dependent on their swimming morphology and phenotypic plasticity (Binning and Roche, 2015, Binning *et al.*, 2014, Fulton *et al.*, 2013). For example, damselfish (*Acanthochromis polyacanthus*) collected from exposed, high wave-energy sites had a 36% larger aerobic capacity and 33% faster critical swimming speed than those that were collected in sheltered locations (Binning *et al.*, 2014). Furthermore, species assemblage, swimming mode and intraspecific phenotypic plasticity have all been linked to environmental water flow characteristics (Binning and Roche, 2015, Fulton and Bellwood, 2005, Fulton *et al.*, 2013, Marcoux and Korsmeyer, 2019). Because many coastal areas are directly vulnerable to changes in wave climate, species that are not capable of adapting to increases in storm surge and wave amplitudes may be forced to move to less suitable habitat if sheltering is not a sustainable option (McCarthy *et al.*, 2001). Therefore, as climate change alters water flow in coastal habitats, concomitant challenges of other anthropogenic effects such as ocean warming and overfishing may result in declining biodiversity and coastal ecosystem function (Bellwood *et al.*, 2003, Hooper *et al.*, 2005, Johansen and Jones, 2011, Micheli *et al.*, 2014).

Obtaining accurate values of energetic requirements for fish is crucial for estimating both short- and long-term energy budgets to predict how species will fare under current and future climate scenarios. Potential costs associated with oscil-

latory, wave-driven water flows are often overlooked due to the difficulty of creating these types of flows in a swimming respirometer. Marcoux and Korsmeyer (2019) were the first to demonstrate the importance of using a cyclical, bidirectional swimming to compare metabolic rates across swimming modes of coral reef fishes. More recently, Schakmann *et al.* (2020) evaluated how the net costs of swimming change with different cyclical flows and found turning was energetically expensive for the labriform swimming, tropical coral reef fish *C. strigosus*. By comparing three different swimming protocols: unidirectional cyclical flow, bidirectional cyclical flow and steady, constant flow, the present study reports the costs of swimming and turning for a temperate labriform swimmer *C. aggregata* in cyclical flows. Along with previous studies, our results indicate a general risk of underestimating  $\dot{M}O_2$  demand for field conditions, especially for species inhabiting dynamic coastal or coral reef ecosystems where swimming is needed in order to maintain station against currents and wave surge (Marcoux and Korsmeyer, 2019, Schakmann *et al.*, 2020). Therefore, the inclusion of increased energetic costs associated with wave surge conditions in the wild may be beneficial in future studies. In addition, comparing species with different swimming modes in both a bidirectional flow and a steady, constant flow is needed to investigate how costs of turning may vary amongst species and could explain why MPF swimming species are common in wave-swept habitats (Fulton, 2007, Fulton and Bellwood, 2005, Fulton *et al.*, 2013); an understanding that is critical for accurate bioenergetic modelling and its use in conservation efforts.

In addition to changes in wave height and intensity, marine fishes also face increases in metabolic rates with increasing sea surface temperatures, leaving many fish in coastal and coral reef ecosystems precariously vulnerable (Johansen and Jones, 2011, Rummer *et al.*, 2014). Underscoring this idea, Johansen and Jones (2011) found a decrease in swimming performance of multiple genera of coral reef damselfishes with increasing water temperature; highlighting that increasing temperatures in conjunction with increasing wave action could compound on the ability of fish to maintain spatial position on wave-swept reefs. Taking into consideration the increased costs associated with station holding found in this study and Schakmann *et al.* (2020), fishes exposed to future increases in temperature may not have the aerobic capacity or the swimming performance needed to stay resident (Johansen and Jones, 2011). Temperature, swimming performance and environmental dynamics all have influence on the energetic requirements of fish in coastal marine ecosystems and therefore need to be considered when developing energy budgets for species that inhabit them.

We conclude that the increased  $\dot{M}O_2$  of swimming in cyclical flows is most prominently due to the cost of turning and not from accelerating or decelerating, expanding upon work by Schakmann *et al.* (2020) on coral reef fish. This behaviour is particularly critical for station holding where fish orient themselves in the direction of flow, highlighting

the importance of effective manoeuvrability in areas with high wave action, and suggests that fish may need to select areas of high productivity for their gains to offset the added costs of turning (Fulton and Bellwood, 2005).

In an era of climate change, a major contribution to the field of conservation physiology is the development of energy budgets, allowing researchers to predict how animals will react to factors associated with anthropogenic-induced effects (Cooke *et al.*, 2004). In decades to come, the severity of storm-surge and wave action is predicted to increase in coastal areas along with increasing sea surface temperatures (McCarthy *et al.*, 2001, Parry *et al.*, 2007, Slott *et al.*, 2006), demonstrating the need to incorporate added costs associated with dynamic coastal habitats when estimating energetic requirements for both temperate and tropical species (Marcoux and Korsmeyer, 2019, Schakmann *et al.*, 2020).

## Acknowledgements

We would like to thank the 2017 Fish Swimming course for support and assistance with fish collections, as well as Friday Harbor Laboratories for the facilities and technical support on this project. S.M.L. would like to thank her sponsor, Claudia Mills, for her financial support to attend the Fish Swimming course at Friday Harbor Labs, University of Washington, San Juan Island. A.R. would like to thank the Elisabeth and Knud Petersen Foundation for financial support. C.R.G. would like to thank Alex Shapiro and for her financial support to attend the Friday Harbor Lab, fish swimming course. The authors would also like to thank Dr Dominique Roche and an anonymous reviewer for their constructive suggestions that greatly improved the manuscript.

## References

- Beamish FWH (1964) Respiration of fishes with special emphasis on standard oxygen consumption: ii. Influence of weight and temperature on respiration of several species. *Can J Zool* 42: 177–188.
- Bell W, Terhune L (1970) *Water Tunnel Design for Fisheries Research (Technical Report No. 195)*. Ottawa, Ontario: Fisheries Research Board of Canada
- Bellwood DR, Hoey AS, Choat JH (2003) Limited functional redundancy in high diversity systems: resilience and ecosystem function on coral reefs. *Ecol Lett* 6: 281–285.
- Binning SA, Roche DG (2015) Water flow and fin shape polymorphism in coral reef fishes. *Ecol* 96: 828–839.
- Binning SA, Roche DG, Fulton CJ (2014) Localised intraspecific variation in the swimming phenotype of a coral reef fish across different wave exposures. *Oecologia* 174: 623–630.
- Blake R (2004) Fish functional design and swimming performance. *J Fish Biol* 65: 1193–1222.

- Blake R, Chan K (2010) Biomechanics of rheotactic behaviour in fishes. In *Fish Locomotion: an Eco-Ethological Perspective*. Science Publishers, Enfield, pp. 40–61.
- Brett J (1964) The respiratory metabolism and swimming performance of young sockeye salmon. *Can J Fish* 21: 1183–1226.
- Brett J (1972) The metabolic demand for oxygen in fish, particularly salmonids, and a comparison with other vertebrates. *Respir Physiol* 14: 151–170.
- Brett JR (1971) Energetic responses of salmon to temperature. A study of some thermal relations in the physiology and freshwater ecology of sockeye salmon (*Oncorhynchus nerka*). *Am Zool* 11: 99–113.
- Carlson RL, Lauder GV (2011) Escaping the flow: boundary layer use by the darter *Etheostoma tetrazonum* (percidae) during benthic station holding. *J Exp Biol* 214: 1181–1193.
- Chabot D, Steffensen JF, Farrell A (2016) The determination of standard metabolic rate in fishes. *J Fish Biol* 88: 81–121.
- Connell JH (1978) Diversity in tropical rain forests and coral reefs. *Sci* 199: 1302–1310.
- Cooke SJ, Hinch SG, Wikelski M, Andrews RD, Kuchel LJ, Wolcott TG, Butler PJ (2004) Biotelemetry: a mechanistic approach to ecology. *Trends Ecol Evol* 19: 334–343.
- Denny MW (2006) Ocean waves, nearshore ecology, and natural selection. *Aquatic Ecol* 40: 439–461.
- Enders EC, Boisclair D, Roy AG (2003) The effect of turbulence on the cost of swimming for juvenile Atlantic salmon (*Salmo salar*). *Can J Fish Aquat Sci* 60: 1149–1160.
- Finlayson D (2006). The geomorphology of puget sound beaches. *Puget Sound Nearshore Partnership Report No. 2006-02* Was hington Sea Grant Program, University of Washington, Seattle Washington.
- Fulton CJ (2007) Swimming speed performance in coral reef fishes: field validations reveal distinct functional groups. *Coral Reefs* 26: 217–228.
- Fulton CJ, Bellwood DR (2005) Wave-induced water motion and the functional implications for coral reef fish assemblages. *Limnol Oceanogr* 50: 255–264.
- Fulton CJ, Binning SA, Wainwright PC, Bellwood DR (2013) Wave-induced abiotic stress shapes phenotypic diversity in a coral reef fish across a geographical cline. *Coral Reefs* 32: 685–689.
- Green E, Carritt D (1967) Oxygen solubility in sea water: thermodynamic influence of sea salt. *Sci* 157: 191–193.
- Hamner W, Jones M, Carleton J, Hauri I, Williams DM (1988) Zooplankton, planktivorous fish, and water currents on a windward reef face: Great Barrier Reef, Australia. *Bull Mar Sci* 42: 459–479.
- Hart DD, Finelli CM (1999) Physical-biological coupling in streams: the pervasive effects of flow on benthic organisms. *Annu Rev Ecol Evol Syst* 30: 363–395.
- Heatwole SJ, Fulton CJ (2013) Behavioural flexibility in reef fishes responding to a rapidly changing wave environment. *Mar Biol* 160: 677–689.
- Hooper DU, Chapin FS, Ewel J, Hector A, Inchausti P, Lavorel S, Lawton JH, Lodge D, Loreau M, Naeem S (2005) Effects of biodiversity on ecosystem functioning: a consensus of current knowledge. *Ecol Monogr* 75: 3–35.
- Johansen J, Jones G (2011) Increasing ocean temperature reduces the metabolic performance and swimming ability of coral reef damselfishes. *Glob Change Biol Bioenergy* 17: 2971–2979.
- Johansen JL (2014) Quantifying water flow within aquatic ecosystems using load cell sensors: a profile of currents experienced by coral reef organisms around Lizard Island, Great Barrier Reef, Australia. *PLoS One* 9: e83240.
- Johansen JL, Bellwood DR, Fulton CJ (2008) Coral reef fishes exploit flow refuges in high-flow habitats. *Mar Ecol* 360: 219–226.
- Johansen JL, Fulton CJ, Bellwood DR (2007) Avoiding the flow: refuges expand the swimming potential of coral reef fishes. *Coral Reefs* 26: 577–583.
- Korsmeyer KE, Steffensen JF, Herskin J (2002) Energetics of median and paired fin swimming, body and caudal fin swimming, and gait transition in parrotfish (*Scarus schlegelii*) and triggerfish (*Rhinecanthus aculeatus*). *J Exp Biol* 205: 1253–1263.
- Kramer DL, McLaughlin RL (2001) The behavioral ecology of intermittent locomotion. *Am Zool* 41: 137–153.
- Lauder GV, Clark BD (1984) Water flow patterns during prey capture by teleost fishes. *J Exp Biol* 113: 143–150.
- Liao JC (2007) A review of fish swimming mechanics and behaviour in altered flows. *Philos Trans R Soc B, Biol Sci* 362: 1973–1993.
- Marcoux TM, Korsmeyer KE (2019) Energetics and behavior of coral reef fishes during oscillatory swimming in a simulated wave surge. *J Exp Biol* 222: jeb191791.
- Marras S, Killen SS, Lindström J, McKenzie DJ, Steffensen JF, Domenici P (2015) Fish swimming in schools save energy regardless of their spatial position. *Behav Ecol Sociobiol* 69: 219–226.
- McCarthy JJ, Canziani OF, Leary NA, Dokken DJ, White KS (2001) *Climate Change 2001: Impacts, Adaptation, and Vulnerability: Contribution of Working Group II to the Third Assessment Report of the Intergovernmental Panel on Climate Change*. Cambridge University Press The Pitt Building, Trumpington Street, Cambridge, United Kingdom.
- Methling C, Tudorache C, Skov PV, Steffensen JF (2011) Pop up satellite tags impair swimming performance and energetics of the European eel (*Anguilla anguilla*). *PLoS One* 6: e20797.
- Micheli F, Mumby PJ, Brumbaugh DR, Broad K, Dahlgren CP, Harborne AR, Holmes KE, Kappel CV, Litvin SY, Sanchirico JN (2014) High vulnerability of ecosystem function and services to diversity loss in Caribbean coral reefs. *Biol Conserv* 171: 186–194.
- Nelson J (2016) Oxygen consumption rate v. rate of energy utilization of fishes: a comparison and brief history of the two measurements. *J Fish Biol* 88: 10–25.

- Parry M, Canziani O, Palutikof J, van der Linden P, Hanson C (2007) *Climate change 2007: Impacts, Adaptation and Vulnerability. Contributions of Working Group II to the Fourth Assessment Report of the Intergovernmental Panel on Climate Change*. Cambridge University Press The Pitt Building, Trumpington Street, Cambridge, United Kingdom.
- Roche DG, Taylor MK, Binning SA, Johansen JL, Domenici P, Steffensen JF (2014) Unsteady flow affects swimming energetics in a labriform fish (*Cymatogaster aggregata*). *J Exp Biol* 217: 414–422.
- Rummer JL, Couturier CS, Stecyk JA, Gardiner NM, Kinch JP, Nilsson GE, Munday PL (2014) Life on the edge: thermal optima for aerobic scope of equatorial reef fishes are close to current day temperatures. *Glob Change Biol Bioenergy* 20: 1055–1066.
- Schakmann M, Steffensen JF, Bushnell PG, Korsmeyer KE (2020) Swimming in unsteady water flows: is turning in a changing flow an energetically expensive endeavor for fish. *J Exp Biol* 223.
- Shaw E, Allen J (1977) Reproductive behavior in the female shiner perch *Cymatogaster aggregata*. *Mar Biol* 40: 81–86.
- Slott JM, Murray AB, Ashton AD, Crowley TJ (2006) Coastline responses to changing storm patterns. *Geophys Res Lett* 33: L18404.
- Steffensen J, Johansen K, Bushnell P (1984) An automated swimming respirometer. *Comparative Biochemistry and Physiology—Part A: Physiology* 79: 437–440.
- Svendsen MBS, Bushnell P, Steffensen JF (2016) Design and setup of intermittent-flow respirometry system for aquatic organisms. *J Fish Biol* 88: 26–50.
- Team RC (2016) R: a language and environment for statistical computing. *R foundation for Statistical Computing, Vienna*.>
- van der Hoop JM, Byron ML, Ozolina K, Miller DL, Johansen JL, Domenici P, Steffensen JF (2018) Turbulent flow reduces oxygen consumption in the labriform swimming shiner perch, *Cymatogaster aggregata*. *J Exp Biol* 221: 1–11.
- Vijay Anand PE, Pillai NGK (2003) Habitat distribution and species diversity of coral reef fishes in the reefslope of the Kavaratti atoll, Lakshadweep, India. *Mar Biol Ass India* 45: 88–98.
- Webb PW (1984) Form and function in fish swimming. *Sci Am* 251: 58–68.
- Webb PW (1989) Station-holding by three species of benthic fishes. *J Exp Biol* 145: 303–320.
- Webb PW (1994) The biology of fish swimming. In *Mechanics and Physiology of Animal Swimming* (L Maddock, Q Bone J.M.B Rayner , eds), pp 45–62 Cambridge: Cambridge University Press
- Young IR, Zieger S, Babanin AV (2011) Global trends in wind speed and wave height. *Sci* 332: 451–455.